Heliyon 10 (2024) e28606

Contents lists available at ScienceDirect

Heliyon

journal homepage: www.cell.com/heliyon

Research article

Sagittal support rather than medial cortical support matters in geriatric intertrochanteric fracture: A finite element analysis study

Jixuan Liu [a], Yufeng Ge [c], Yu Wang [b], Qing Yang [b], Sutuke Yibulayimu [b], Xinbao Wu [c], Wei Tian [c], Chao Shi [b], Yanzhen Liu [b], Minghui Yang [c,*]

[a] Institue of Medical Equipment Science and Engineering (IMESE), Huazhong University of Science and Technology, Wuhan, 430074, China
[b] School of Biological Science and Medical Engineering, Beihang University, Beijing, 100083, China
[c] Department of Orthopaedics and Traumatology, Beijing Jishuitan Hospital, Capital Medical University, Beijing, China

ARTICLE INFO

Keywords:
Intertrochanteric fracture
Cortex support
Osteo-degenerative features
Biomechanical analysis
Age-specifically

ABSTRACT

Hip fracture, increasing exponentially with age, is osteoporosis's most severe clinical consequence. Intertrochanteric fracture, one of the main types of hip fracture, is associated with higher mortality and morbidity. The current research hotspots lay in improving the treatment effect and optimizing the secondary stability after intertrochanteric fracture surgery. Cortex buttress reduction is a widely accepted method for treating intertrochanteric fracture by allowing the head-neck fragment to slide and rigidly contact the femoral shaft's cortex. Medial cortical support is considered a more effective option in treating young patients. However, osteo-degenerations features, including bone weakness and cortical thickness thinning, affect the performance of cortex support in geriatric intertrochanteric fracture treatment. Literature focusing on the age-specific difference in cortex performance in the fractured hip is scarce. We hypothesized that this osteo-19 degenerative feature affects the performance of cortex support in treating intertrochanteric fractures between the young and the elderly. We established twenty models for the old and the young with intertrochanteric fractures and performed static and dynamic simulations under one-legged stance and walking cycle conditions. The von Mises stress and displacement on the femur, proximal femoral nail anti-rotation (PFNA) implant, fracture plane, and the cutting volume of cancellous bone of the femur were compared. It was observed that defects in the anterior and posterior cortical bone walls significantly increase the stress on the PFNA implant, the displacement of the fracture surface, and cause a greater volume of cancellous bone to be resected. We concluded that ensuring the integrity and alignment of the anterior and posterior cortical bones is essential for elderly patients, and sagittal support is recommended. This finding suggests that the treatment method for intertrochanteric fracture may differ, considering the patient's age difference.

1. Introduction

Hip fracture, which grows exponentially with age, is the most severe clinical consequence of osteoporosis and causes a significant financial burden on the public health care system [1–3]. These fractures are linked to a 10%–20% mortality risk, functional disability,

* Corresponding author.
E-mail address: doctyang0125@126.com (M. Yang).

https://doi.org/10.1016/j.heliyon.2024.e28606
Received 2 March 2023; Received in revised form 20 March 2024; Accepted 21 March 2024

and mobility loss([4,5]). By 2050, hip fractures will affect up to 6.3 million individuals worldwide, including 3.25 million in Asia [6]. Intertrochanteric fracture (ITF), one of the most common types of hip fracture, is associated with higher mortality and morbidity ([7, 8]). Surgical treatment with intramedullary implants has been advocated for treating ITF, during which reduction quality should be the foremost priority. Among several implant types, proximal femoral nail anti-rotation (PFNA) is considered a suitable internal fixation implant and has a more effective therapeutic impact in treating ITF than other internal fixators [9–11].

Alignment, angulation, and cortical bone apposition were widely examined for intraoperative and postoperative evaluations of fracture reduction quality. Gottfried introduced the concept of nonanatomic medial cortical buttress reduction between the proximal and distal fracture components to facilitate secondary fracture healing stability after surgery ([12,13]). Based on Gottfried's results, Chang et al. ([14,15])proposed the concept of positive anteromedial cortical support reduction for unstable pertrochanteric fractures. According to this theory, head-neck fragments' medial and anterior cortical bones were misaligned positive to the femur shaft. They believe the anteromedial cortex's misalignment prevents fracture sliding and provides support for secondary fracture healing. Shao et al. [16] also determined that the anteromedial cortical support reduction pattern exhibited improved mechanical stability for unstable pertrochanteric fractures through finite element analysis. Mao et al. [17] constructed in-silico and biomechanical models for both positive medial cortical support and anatomical reduction, concluding that positive medial cortical support is more effective in treating unstable trochanteric hip fractures. In addition, clinical retrospective research was also performed to justify the anticipated mechanical advantages of medial cortical support([16,18–20]). Ramachandran et al. investigated prospectively 72 patients with unstable pertrochanteric fractures treated with PFNAs. Only 4% of patients with medial cortical support reduction had a mechanical failure, whereas 31% percent with lateral cortical support reduction had a mechanical failure [19].

ITF is closely associated with osteoporosis. Age-related changes will occur in the bone density and cortical bone thickness of the elderly. Ward et al. [21] reported that the cortical bone thickness of those older than 50 decreased by 14% every decade. Riggs et al. [22] found that bone density declines with age, especially in older adults with osteoporosis, resulting in changes to the bone's mechanical strength against loading force. We anticipated that this osteo-degenerative trait affects the effectiveness of cortex buttress support in treating ITFs. There exists a notable gap in biomechanical studies addressing this concern. Existing research typically bases simulations on the bone parameters of younger individuals, overlooking the pronounced bone deterioration that contrasts the elderly from the young. Additionally, prevailing treatment protocols fall short in offering distinct approaches for intertrochanteric fractures depending on age groups. Therefore, it is imperative to investigate if these osteo-degenerative properties, such as bone fragility and decreasing cortical bone thickness, affect the efficacy of cortex buttress support in ITF treatment.

The finite element (FE) method has been used extensively in biomechanics research. Many conditions that would be difficult or impossible to research in reality may be simulated ([23,24]). We used the FE method to examine the biomechanical characteristics of

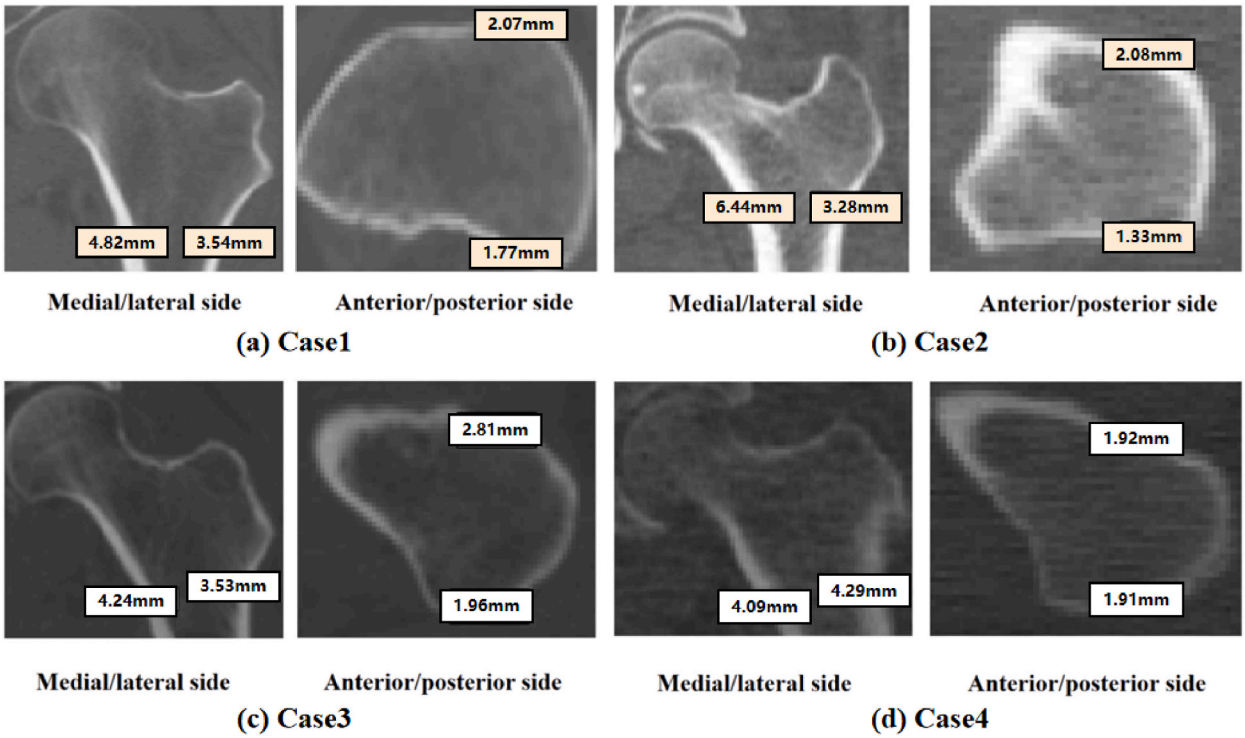

Fig. 1. We measured the cortical thickness of the anterior, posterior, medial, and lateral sides of the femoral trochanter in 4 patients aged under 60. (a) Cortical thickness measurement of case 1, with the left panel showing the thickness of the medial and lateral sides, and the right panel showing the anterior and posterior sides. (b), (c), and (d) depict the cortical thickness measurement of case 2, 3, and 4, respectively.

ITFs with neutral, medial, lateral, and anterior cortical supports in different age groups. A static simulation of a one-legged stance and a dynamic simulation of walking is performed. Twenty model groups were developed in all. Both the elderly and the young had five cortical support models in the static and dynamic simulations. We analyze the Von Mises stress distribution and displacement of bone pieces and fracture plane in the static simulation, as well as the cancellous bone cutting volume throughout a gait cycle in the dynamic simulation model. These analyses were employed to elucidate the influence of osteo-degenerative characteristics on the clinical outcomes of employing a cortical buttress reduction strategy.

2. Method

2.1. Age-specific model configuration and materials properties

Age has a considerable effect on the bone's biomechanical qualities. Cortical bone, once reasonably stable in bone properties, would be lost and damaged beyond age 60 [20,21]. In the current research, 60 years is the dividing line between young and old models, after which cortical bone content falls progressively. Therefore, we set the age of the young model to be under 60 and the elderly model to be about 70. For the assignment of cortical bone thickness in young model, we measured the cortical bone thickness on the anterior, posterior, medial, and lateral sides of the femur for patients used in model reconstruction. In addition to this, we collected data from three other patients under the age of 60 who had similar types of fractures for femoral cortical bone thickness measurements, aiming to improve the precision of cortical bone thickness assignment in this study, seen as Fig. 1. Table 1 has the specific values. The selection criteria for these cases were primarily based on having similar AO/OTA Type A1 intertrochanteric fractures, with age being our main reference factor, and the absence of other comorbid conditions. The anterior cortical bone thickness was the thinnest, with a mean value of 1.74 mm among the four patients. The median value for the thickness of the medial cortical bone was 4.90 mm. In order to control variables and simplify the model, the mean thickness of medial, lateral, anterior, and posterior cortical bone was averaged and was determined to be 3.13 mm.

The assignment of cortical bone thickness for the elderly model was based on the work of Lu Yin et al. [25]. They received CT scans from the hospital of 194 70-year-old women and found that the average thickness of cortical bone around the femoral trochanter was 1.77 $\pm$ 0.29 mm. Therefore, we assigned 2 mm as the cortical bone thickness in the fracture model for the elderly. The numerical values of material attributes differ between the old and young models. Normal cortical and cancellous bone have elastic moduli of 15,1 GPa and 445 MPa, respectively. Cortical and cancellous elastic modulus in osteoporotic bone would be lowered by 33% and 66%, respectively [26–29]. These values were based on calculations relating reported bone mineral density (BMD) measurements in healthy and osteoporotic bone to Young's moduli. Therefore, we assigned the elastic modulus for the old model with a value of 10.117 GPa for cortical bone, 150 MPa for cancellous bone, and a Poisson's ratio of 0.3. Table 2 displays the model's material attributes.

2.2. Establishment of the finite element models

Fig. 2 (a) depicts the building procedures for modeling five forms of cortical support in treating ITFs. First, we collected from Beijing Jishuitan Hospital a set of high-resolution computed tomography (CT) patient data (a 57-year-old Chinese woman, 169 cm, 48 kg) with a slice thickness of 0.67 mm. This collection of CT data is imported into MIMICS software (Materialize, Leuven, Belgium) to rebuild the geometry of her femur based on the tissue's gray value and the area segmentation. Second, the rebuilt model file was imported into Geomagics Studio for additional processing and the generation of non-uniform rational B-spline (NURBS)-wrapped surfaces. In the Geomagics program, we additionally segmented the cortical and cancellous bone and rebuilt the cancellous bone using the offset command. The offset distance is set at 4 mm, and this choice is based on previous research literature [16] and clinical recommendations that suggest the offset displacement should be 1.5 to 2 times the cortical bone thickness. According to the perspective of clinical doctors, an offset difference of half to one cortical bone is still considered anatomical reduction. Therefore, we ultimately decided on a reduction deviation of two cortical bones, which is approximately 4 mm. Thirdly, the model file was loaded into SolidWorks (DASSAULT SYSTEM, FRANCE) to reconstruct ITF patterns. The chosen fracture pattern for this study corresponds to the A1 type of intertrochanteric fractures. This specific type highlights the most preserved cortical bone wall when compared to other fracture types, as evidenced by its clearly delineated fracture line [30]. We created two sets of ITF models, one for the old and one for the young. Cortical bone thickness is one of the distinctions between young and elderly models, seen as Fig. 2 (b). Each model set

Table 1
Cortical bone thickness measurements on the anterior, posterior, medial, and lateral sides of the intertrochanteric region in 4 patients, along with the averages for each side and the overall mean.

	Cortical bone thickness around the femoral trochanter for young(mm)			
	Medial	Lateral	Anterior	Posterior
Case 1	4.82	3.54	1.77	2.07
Case 2	6.44	3.28	1.33	2.08
Case 3	4.24	3.53	1.96	2.81
Case 4	4.09	4.29	1.91	1.92
Average value	4.90	3.66	1.74	2.22
Average all	3.13			

Table 2
Material attributes assigned to cortical bone, cancellous bone, and the PFNA implant in both elderly and young patient models.

Material	Density(g/cm^3)	Young's Modulus (Mpa)	Poisson's ratio
Cortical bone(old)	1.38	10117	0.3
Cancellous bone(old)	0.45	150	0.2
Cortical bone(young)	1.38	15100	0.3
Cancellous bone(young)	0.45	445	0.2
PFNA-II(Ti–6Al–7NB)	4.43	110000	0.3

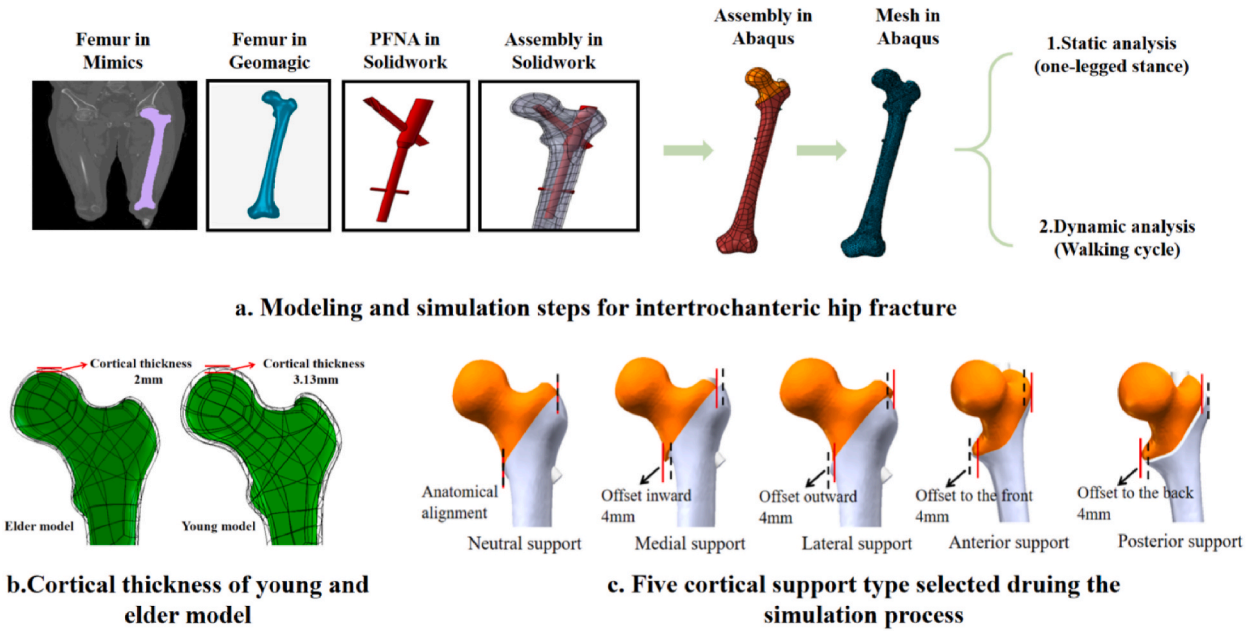

Fig. 2. Construction steps for modeling the intertrochanteric fractures (a), the distinction between elderly and young models regarding the cortical thickness(b), and the illustration of five cortical support in ITFs treatment(c).

consists of fractures of the neutral, anterior, posterior, medial, and lateral cortical supports, seen as Fig. 2 (c). The neutral support places bone fragments in their anatomical location. Correspondingly, the medial, lateral, anterior, and posterior cortical supports represent the head-neck segments displaced 4 mm from the femoral shaft inwards, outwards, forwards, and backwards. This choice of 4 mm aligns with the recommendation that it should be approximately 1.5–2 times the cortical bone thickness.

The PFNA-II (DePuy Synthes, Raynham, MA) model was also developed in Solidworks, including a helical blade, an intramedullary nail, and distal locking screws. The geometrical parameters of the PFNA-II were taken from the implant manufacturer's catalog (length 170 mm, width 11 mm, 5°proximal lateralization angle, helical blade length 95 mm, center-column-diaphyseal (CCD) angle 130°). Then, 20 fractured models and the PFNA-II model were assembled, and the tip-apex distance (TAD) was adjusted to within 20 mm. These models were then loaded into Abaqus (DASSEILLE SYSTEM, FRANCE) for subsequent static and dynamic analysis (one-legged stance and walking cycle).

2.3. Model validation

CristofoIini's biomechanical testing on composite synthetic models and cadaveric bones served as the basis for validating the material characteristics and mesh sizes used in our models before the finite element simulation [31]. In the investigation conducted by CristofoIini, the composite synthetic femur and two types of cadaveric bone (including the fresh-frozen femur and the dried rehydrated femur) were subjected to various external loading conditions. We replicated their experimental conditions and assessed the distribution of bone strain in the medial femoral wall cortex. In accordance with the arrangement of five strain gauges (M1-M5) used in the experiment, Fig. 3 (a) illustrates the minimum principal strain at the M1-M5 sites. These sites were evaluated across various scenarios, including the young femur model (consistent with CristofoIini's experiment), elderly femur model, young femur model with PFNA, and elderly femur model with PFNA simulations.

We selected two sets of experimental strain measurements from CristofoIini's literature [31], namely 'Composite Femur' and 'Cadaveric Femur #24,' and compared them with the data obtained from our finite element model, referred to as the 'FE young model', as seen in Fig. 3 (b). We calculated the mean strain values, medians, and standard deviations for each dataset and conducted an analysis

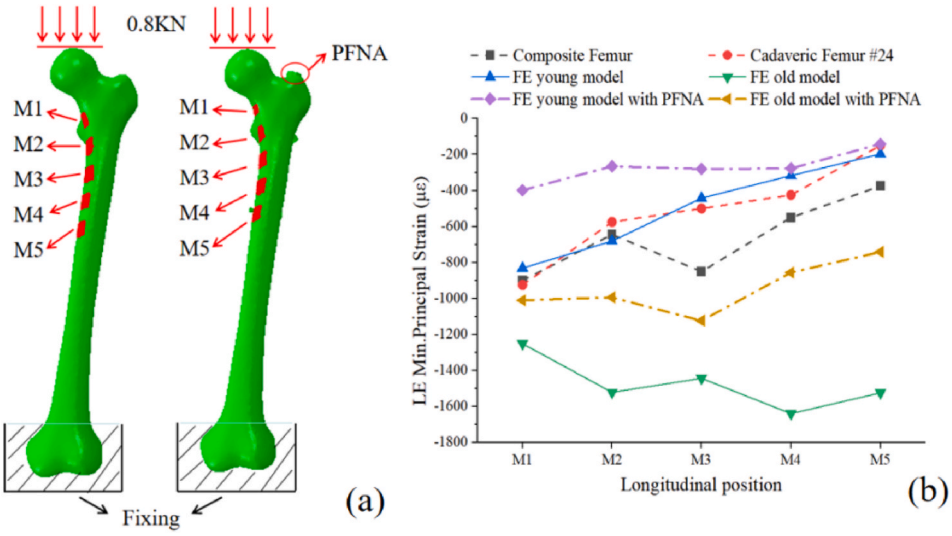

Fig. 3. We validated the established ITF models based on the experimental results of CristofoIini et al. [31]. (a) Illustrates the mechanical experiments conducted by CristofoIini et al. on cadaveric bone and synthetic bone, including the setup for load application and femoral medial strain sensors. (b) Presents a comparison between the minimum principal strains measured in the mechanical experiments (M1-M5 strain sensors) and the simulation results of our model (in units of micro-strain με). Additionally, we included mechanical simulations of PFNA implant fixation on the femur, the results of which are also shown in (b). "FE" stands for Finite Element Analysis.

of variance (ANOVA) to assess whether there were significant differences in the distributions of the three datasets. The results are presented in Tables 3 and 4.

Table .4 presents the analysis of variance (ANOVA) for the strain factor, detailing the sum of squares, degrees of freedom (df), mean square, F-value, and significance (Sig.) across different groups (Between Groups) as well as within each group (Within Groups). The significance level of 0.53(> 0.05), indicates that there is no significant difference between groups.

Based on the analysis of minimum principal strain in the young model (represented by the blue solid line), which is consistent with the experimental data of CristofoIini (depicted by the red and black dashed lines), it is evident that the strain change trend and values closely align. In the analysis of variance table (Table 4), the significance level for between-group data is 0.530. This suggests that there is no significant difference in the distributions among the three datasets. Therefore, we conclude that the simulated results obtained by the model in this study are consistent with the experimental measurements, validating the effectiveness of the model presented in this paper.

Additionally, it is worth noting that the strain observed in the femur of the elderly model is significantly greater than that in the young model (solid green line). This indicates that under the same load, the elderly model will experience more significant deformation of the femur compared to the young model. However, after PFNA assembly, the strain magnitude on the femur may be greatly reduced (purple and orange dash-dotted lines), and the strain values at points M1-M5 tend to become more stable."

2.4. Load force setting under static and dynamic analysis

Based on the experimentally validated FE model of ITFs, we conducted follow-up studies to investigate the mechanical stability performance of five different types of cortical bone support reduction in both elderly and young individuals. These studies were performed under both static and dynamic mechanical loading conditions. Static analysis corresponds to the standing posture of patients after surgery, while dynamic analysis relates to their post-surgery walking activities. These activities are representative of the inevitable daily activities for patients with intertrochanteric fractures postoperatively.

In the statics analysis, the load force setting refers to the one-legged stance force distribution on the proximal femur reported by Lotz et al. [32].This encompasses the forces exerted by the hip (self-gravity) and the gluteus medius muscle, as depicted in Fig. 4(a). Table 5 displays the force load (multiples of body weight) and unit vectors for the XYZ coordination system (as per CT output). For the

Table 3
Descriptive Statistical Analysis of strain value for Composite Femur, Cadaveric Femur #24, and FE young model.

Source	Mean Strain	N	Std. Deviation	Median Strain	Std. Error of Mean
Composite Femur	−664.0000	5	216.31574	−645.0000	96.73934
Cadaveric Femur #24	−515.0000	5	279.84371	−500.0000	125.14991
FE young model	−493.8140	5	259.87785	−442.6000	116.22091
Total	−557.6047	15	247.35571	−550.0000	63.86697

Table 4
Analysis of Variance for Composite Femur, Cadaveric Femur #24, and FE young model.

			Sum of Squares	df	Mean Square	F	Sig.
Strain * Source	Between Groups	(Combined)	86021.869	2	43010.934	0.670	0.530
		Linearity	72408.186	1	72408.186	1.128	0.309
		Deviation from Linearity	13613.682	1	13613.682	0.212	0.653
	Within Groups		770565.991	12	64213.833		
	Total		856587.859	14			

dynamic analysis, the load force setting refers to the work of Bergmann [33] et al., demonstrating that the surface contact force of the unilateral hip joint varies during walking. Fig. 4 (b) illustrates the loading point and direction at the hip joint surface.

A total of 20 model groups entered the post-processing (result analysis) phase of the finite element analysis. These models are categorized based on two age groups (elderly and young), two types of mechanical loading (static and dynamic), and five types of cortical bone support reduction methods (medial, lateral, anterior, posterior, and neutral), resulting in a total of 2*2*5 = 20 models.

3. Results

In static analysis, the Von Mises stress distribution, the peak value stress on the femur and PFNA, and the fracture plane's maximum displacement were measured and compared. In dynamic analysis, the fracture plane's maximum principal strain and the minimum principal strain of cancellous bone were compared.

3.1. Static analysis results

3.1.1. Peak value stress on the femur and PFNA

Fig. 5 shows the maximum stress values on the femur and PFNA implants in the old and young models with five cortical bone supports. The specific values are listed in Table 6.

As shown in Fig. 5 and Table 6, the average peak von Mises stress of the young model on the femur under the five cortical support types is 421.92Mpa, whereas the average peak von Mises stress of the old model is 380.38Mpa. The average peak von Mises stress on the PFNA implant (the intramedullary nail, the distal screw, and the helical blade) for the young model is 133.00Mpa, 82.82Mpa, and 30.40Mpa, respectively. The old model's average peak von Mises stress on PFNA implants is 280.14Mpa, 156.63Mpa, and 61.99Mpa. For the old model, the weight bearing on the femur is lower than that of young people due to the weakness of bone strength, whereas the weight bearing on the PFNA is higher than that of young people.

In the young model, the medial cortical support performed better, and the maximum stress on the femur was minimal. However, in the old model, it was observed that the posterior cortical support, corresponding to the anterior cortical bone defect, produced a significant increase in stress on the intramedullary nail.

3.1.2. Stress distribution on the femur and PFNA

Then, using the finite element method, we constructed the von Mises stress distribution nephogram for the femur and the PFNA implant, as shown in Figs. 6 and 7. To facilitate results comparison, we unified the scale of the legends, setting it to 0–100 MPa. The

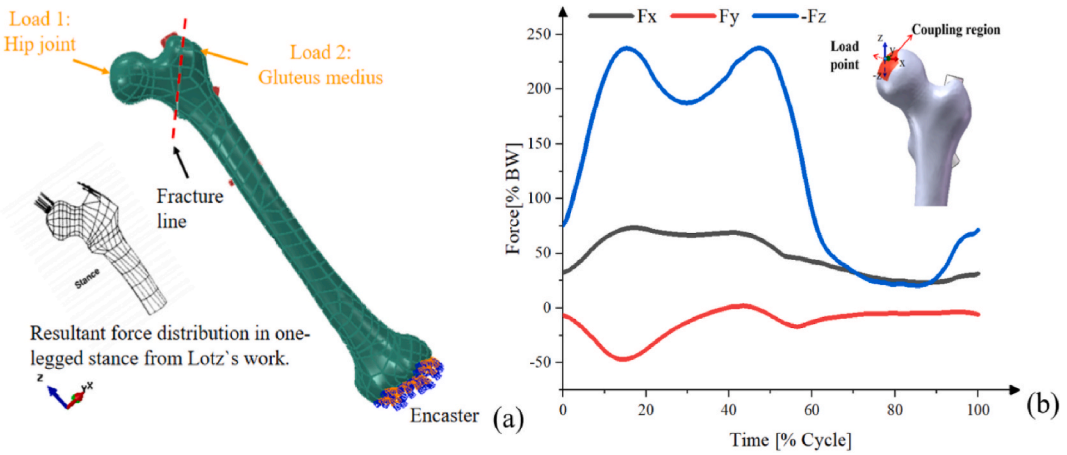

Fig. 4. In the static simulation of the model, the application of mechanical loads is based on the research by Lotz [32], which simulates a composite hip joint load at the femoral head and a gluteus medius load at the lateral side of the femoral trochanter (a). In the dynamic simulation, the load application follows the work of Bergmann [33], involving a dynamic load applied to the femoral head that varies with the gait cycle(b).

Table 5
Load magnitude in static simulation (multiples of body weight, 480 N) and direction of force application.

Force location	One-legged stance(multiple)	Force direction (x, y, z)
Load 1: Hip joint	1.80	(0.29,-0.10,-0.95)
Load 2: Gluteus Medius	2.60	(-0.40,-0.14,0.91)

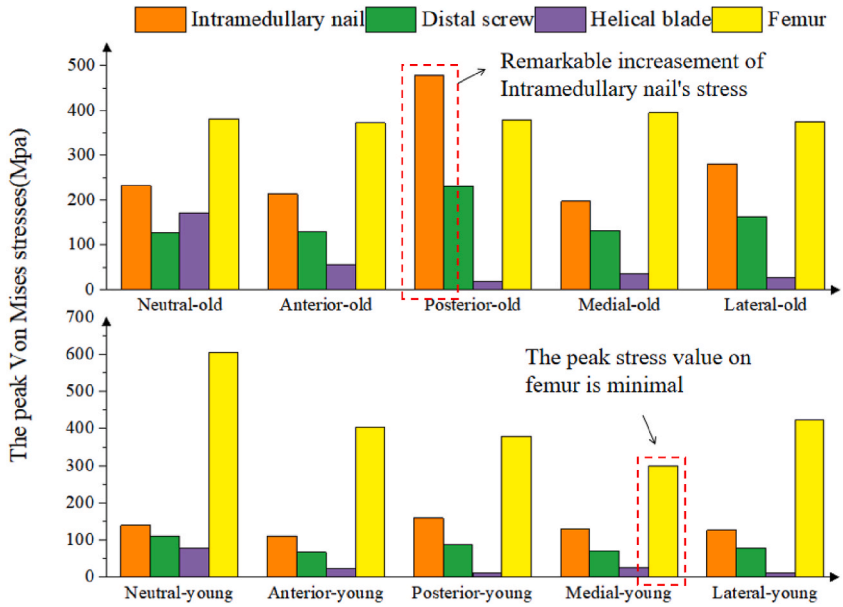

Fig. 5. The peak von Mises stresses on the femur and PFNA implants. In the elderly model, the stress on the PFNA intramedullary nail increases sharply with the posterior cortical bone support, which can enhance stress shielding and affect subsequent fracture healing. In the model of young individuals, the medial cortical bone support demonstrates a greater advantage, with the stress on both the PFNA and the femur being the minimal.

Table 6
The specific peak von Mises stress values of the femur and the PFNA implant, as well as the average stress value under five cortical bone support conditions.

Model and support type	Intramedullary nail (Mpa)		Distal screw (Mpa)		Helical blade (Mpa)		Femur (Mpa)	
	Young	Old	Young	Old	Young	Old	Young	Old
Neutral	139.00	232.03	111.00	127.44	77.70	171.49	603.70	381.60
Anterior	110.00	214.15	66.80	129.31	23.60	56.31	403.70	372.00
Posterior	159.00	476.54	89.00	230.87	11.80	19.41	378.50	378.90
Medial	130.00	197.32	70.40	132.59	26.80	35.02	299.60	394.30
Lateral	127.00	280.65	76.90	162.95	12.10	27.70	424.10	375.10
Average value	133.00	280.14	82.82	156.63	30.40	61.99	421.92	380.38

dark blue region corresponds to a pressure of around 0Mpa, whereas the green and light green regions reflect a pressure range of 50Mpa. The area above 100 MPa and up to the maximum stress value is the high-stress zone, shown in dark red. The reasons for setting the stress regions in this way will be explained in the discussion section.

The stress distribution nephogram reveals that, on both the femur bone and the PFNA, the stress distribution dramatically increases once the anterior and posterior cortical bone support is misaligned in the old model, and enormous high-stress zones arise. In contrast, no similar behavior is found in the young model, and the stress distributions on the femur and PFNA are comparable across the five cortical support forms. We conclude that sagittal support is vital for treating ITFs in older people. The integrity and alignment of the anterior and posterior lateral walls, i.e., sagittal plane support, are of greater concern to these patients.

3.1.3. Displacement of femur and fracture plane

Fig. 8 depicts the displacement nephogram on the femur, the maximum displacement of the femur, and the relative displacement between two bone fragments on the fracture plane. For the young model, the displacement generated by medial and lateral cortical support was minimal at 0.95 mm and 0.81 mm, respectively. The neutral cortical support generated a maximum displacement of 1.3 mm, which is the maximum. In addition, neutral cortical support produced 0.23 mm relative displacement of the fracture plane, about

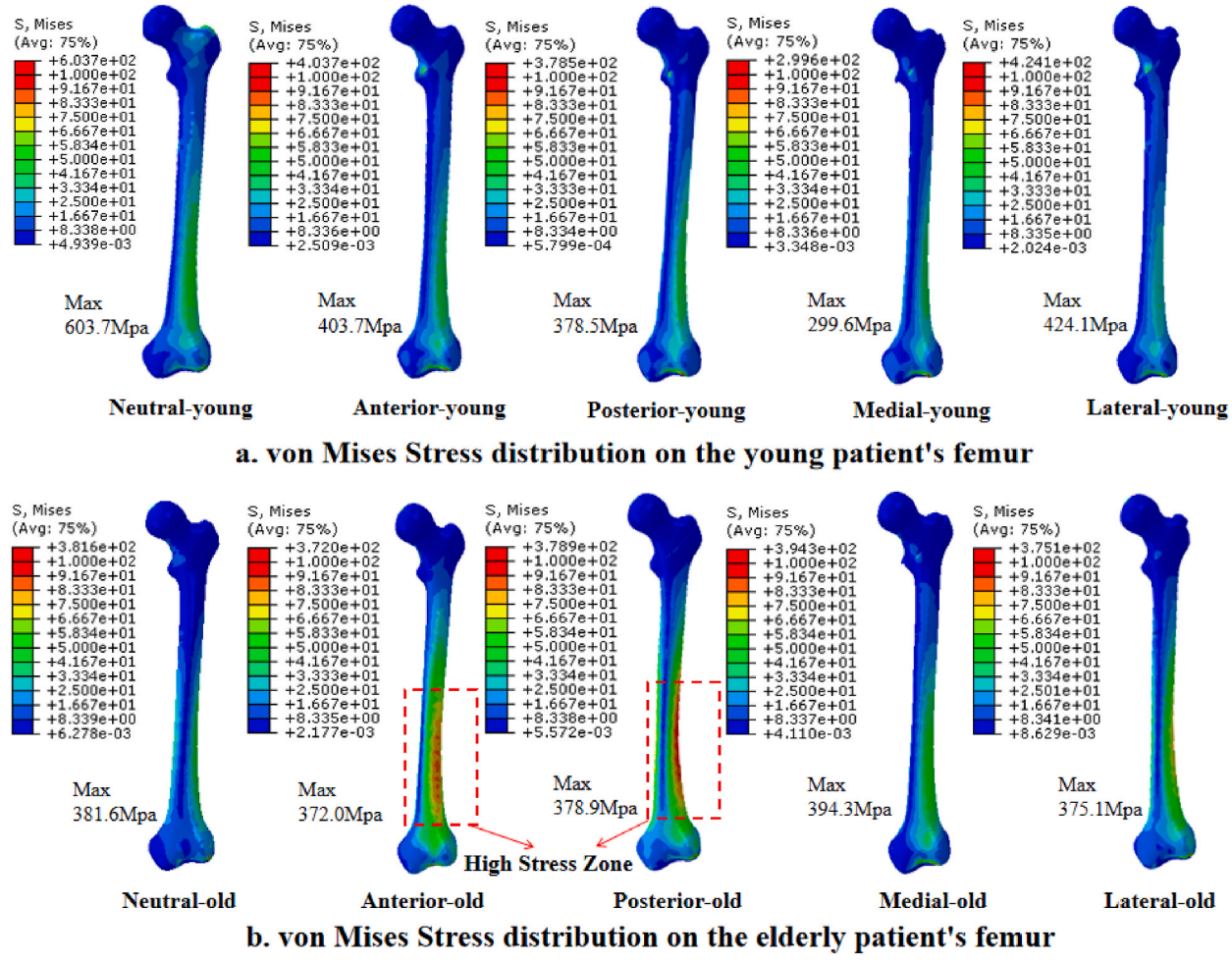

Fig. 6. Von Mises Stress distribution on the young (a) and elderly (b) femur under five cortical support conditions.The stress distribution nephogram is scaled from 0 to 100 MPa, with areas exceeding 100 MPa designated as high-stress zones, highlighted in red. In the elderly model, both anterior and posterior cortical bone support conditions lead to widespread stress concentration (red areas) in the distal screw fixation region of the femur, a situation not observed in the young individual's model.

100 times that of the medial cortical support (0.038 mm, the minimum value). The less the relative displacement of the fracture plane, the more stable and advantageous the anticipated postoperative outcome. This suggests that medial cortical support performed good postoperative stability in young people. The relative displacement of the other three cortical supports (anterior, posterior, and lateral) was less than 1 mm.

For the old model under the five cortical supports, the medial cortical bone support caused the least displacement (16.76 mm of the femur and 0.55 mm of the fracture plane). Like stress distribution, when the anterior and posterior cortical bones became misaligned, the displacement of the femur and fracture planes increased dramatically (34.05 mm and 3.04 mm under anterior cortical support and 36.89 mm and 3.4 mm under posterior cortical support). Due to bone fragility and cortical thinning, the old model's displacement is much greater than that of the young model. For older people, more attention should be paid to the effects of anterior and posterior cortical walls' integrity and alignment, illustrating the importance of sagittal support.

3.2. Dynamic analysis results

3.2.1. The maximal principal strain on the fracture plane

Dynamic analysis reveals the influence of cumulative strain on mesh elements throughout force loading time. Fig. 9 demonstrates the maximum principal strain on the fracture plane. The red zone represents tensional strain (a positive strain value), while the blue zone represents compressive strain (a negative strain value). In most instances, the normal compressive strain was shown to be beneficial for bone healing [34]. However, bone cutting is possible when the compressive strain value is less than the yield strain limit of cancellous bone (−0.8%) [35]. The green area represents the region that will likely be removed. In young models, the medial and neutral cortical bone supports have the greatest compressive strain area. In old models, it is difficult to visibly compare the compressive

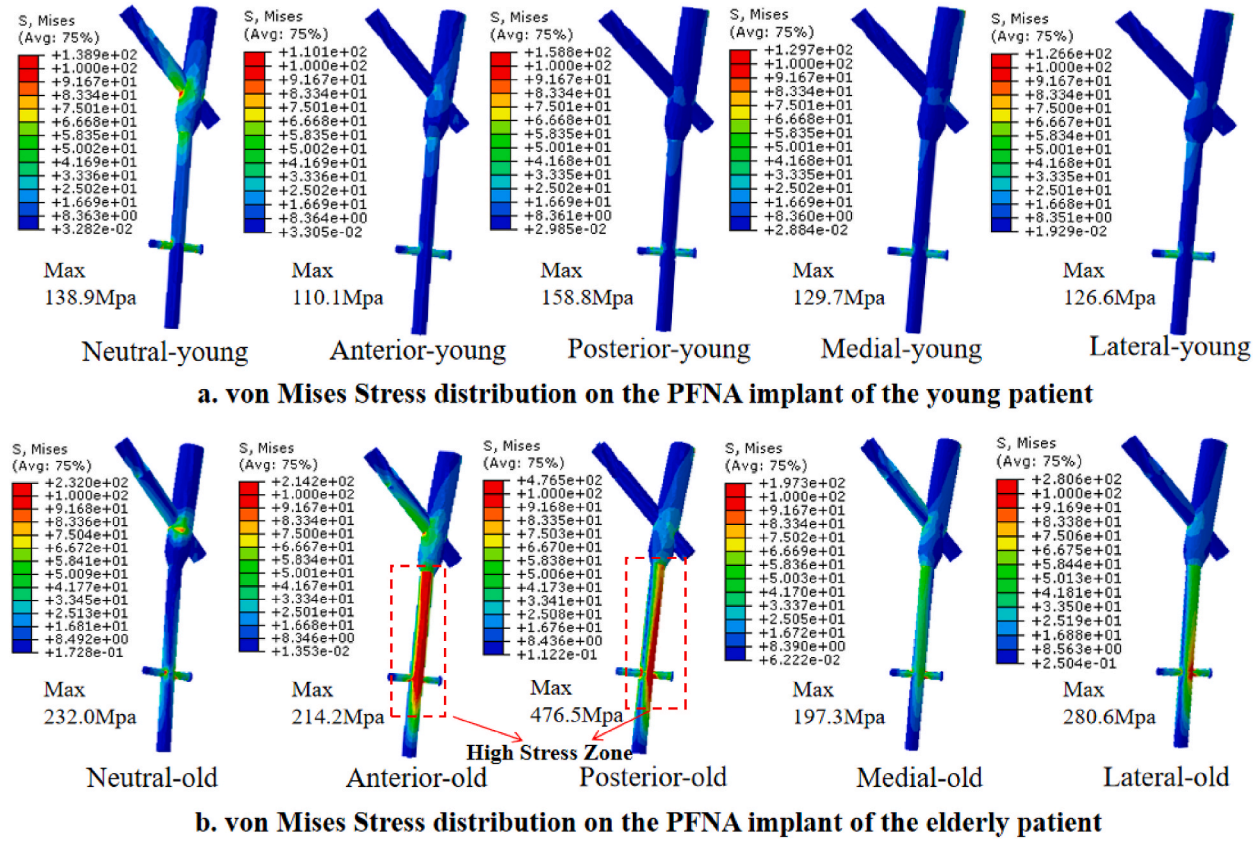

Fig. 7. Von Mises Stress distribution on the PFNA implant of the young (a) and elderly (b) patients under five cortical support conditions. In the elderly model, the distal screw fixation region of the PFNA shows a large area of red (high-stress zone) under both anterior and posterior cortical bone support conditions, while in the young model, this is not observed. The scale of the stress distribution nephogram ranges from 0 to 100 MPa.

strain region of the five cortical bone supports. However, bone cutting out is an issue with anterior, posterior, and lateral cortical supports, particularly with posterior cortical support.

3.2.2. The minimal principal strain of the femur

Fig. 10 displays the minimum principal strain derived from the femur's dynamic study. The yield strain of cancellous bone is −0.8%. We calculated the bone-cutting volume of each model with a strain less than −0.8%. The medial cortical support resulted in the smallest amount of cancellous bone removal cutting in both the young and old models (113 mm^3 and 291 mm^3, respectively). In the old models, the cutting volumes of anterior (1113 mm^3) and posterior (2069 mm^3) cortical support are much greater than the medial cortical support volume (291 mm^3). This indicates that once the anterior and posterior cortical bones are misaligned, the effectiveness of ITF therapy is greatly diminished.

4. Discussion

Extensive clinical trial data [18–20] and biomechanical simulation analyses have supported the use of medial cortical support in the treatment of ITFs (some sources refer to medial-anterior cortical support) [11–16]. However, information on the effect of age on ITF therapy with cortical bone support has yet to be available. Age increase leads to changes in the bone structure around the trochanter and a deterioration in skeletal strength, which mainly manifested in the decrement of cortical bone thickness and the biomechanical strength of the bone. Due to diminishing cortical bone thickness and deteriorating bone strength, older and younger individuals exhibit distinct skeletal characteristics ([21,22]). Even though medial cortical bone support is still a reasonably effective method for treating ITF in the elderly, the integrity and alignment of anterior and posterior cortical bone should be prioritized. When misalignment and loss of integrity occur in these two components, ITF's therapeutic effectiveness is dramatically compromised. In contrast to ITF treatment for young people, anterior and posterior misalignment does not significantly impair the therapeutic effect. Therefore, for the treatment of ITFs in the elderly, sagittal support may be a more recommended way and the defect of the anterior and posterior cortical walls should be avoided.

In this study, we compared the performance of five cortical bone support reduction performances in older and younger individuals using the finite element approach. Twenty ITF models with PFNA fixation of the old and young groups were developed, and static and

The displacement nephogram of the young model

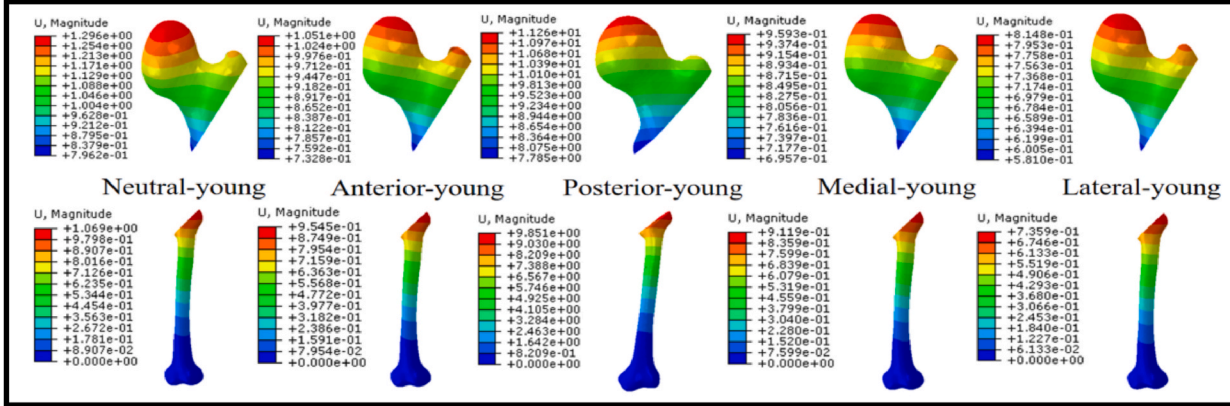

Young model	The maximum displacement on the femur (mm)				
	Neutral	Anterior	Posterior	Medial	Lateral
	1.3	1.05	1.05	0.95	0.81
	The relative displacement on the fracture plane (mm)				
	Neutral	Anterior	Posterior	Medial	Lateral
	0.23	0.096	0.097	0.038	0.08

The displacement nephogram of the old model

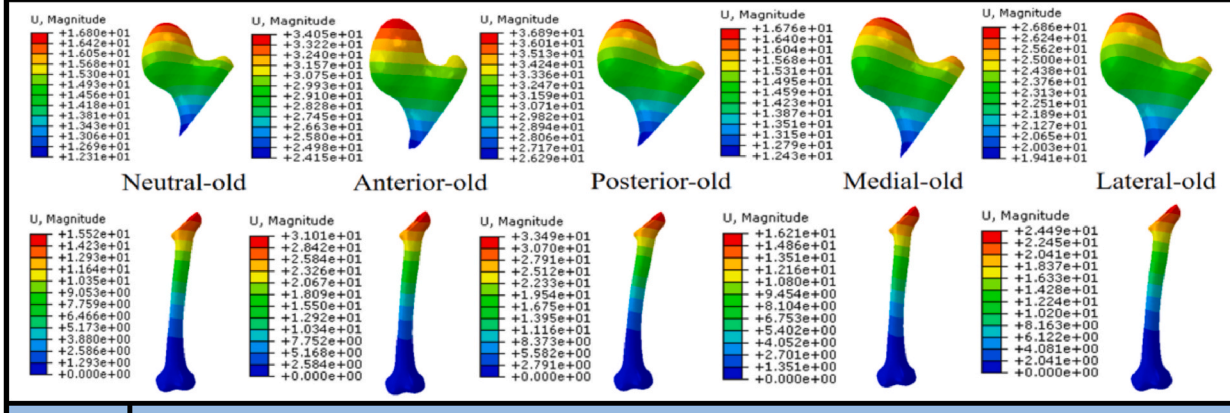

Old model	The maximum displacement on the femur (mm)				
	Neutral	Anterior	Posterior	Medial	Lateral
	16.8	34.05	36.89	16.76	26.86
	The relative displacement on the fracture plane (mm)				
	Neutral	Anterior	Posterior	Medial	Lateral
	1.28	3.04	3.4	0.55	2.37

(caption on next page)

Fig. 8. The maximum displacement, the relative displacement on the fracture plane, and displacement nephogram of the old and young models. In the young model, the maximum displacement on the femur does not show significant differences under the five cortical bone support conditions. However, in the elderly model, the anterior and posterior cortical bone support significantly increases the displacement on the femur, more than twice that of the neutral cortical bone support condition. The relative displacement on the fracture plane follows a similar pattern.

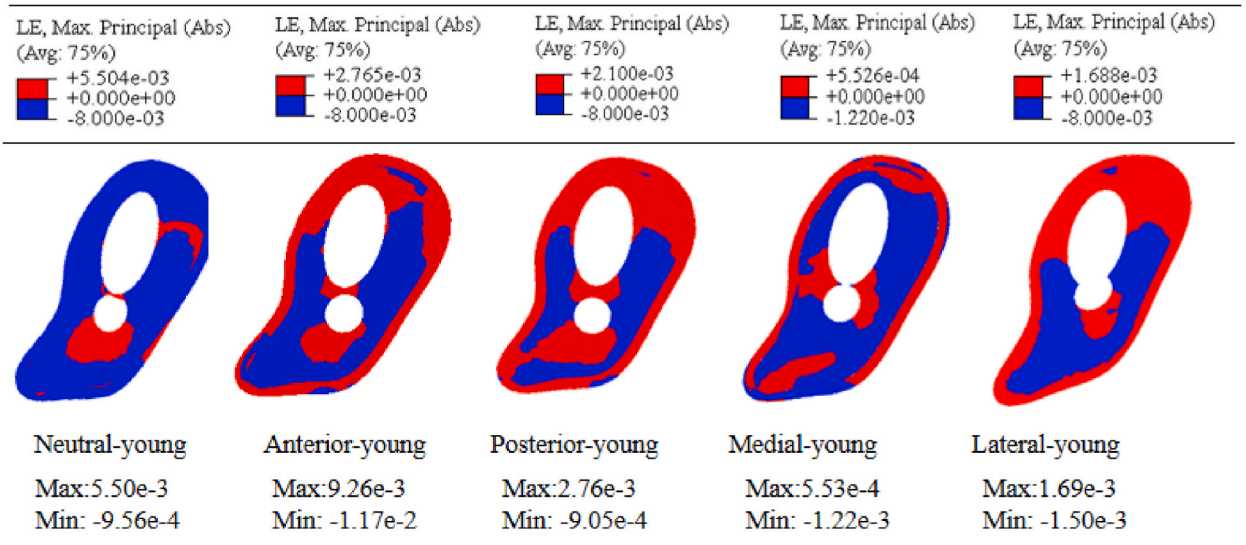

a. The maximal principal strain of the fracture plane of young patient

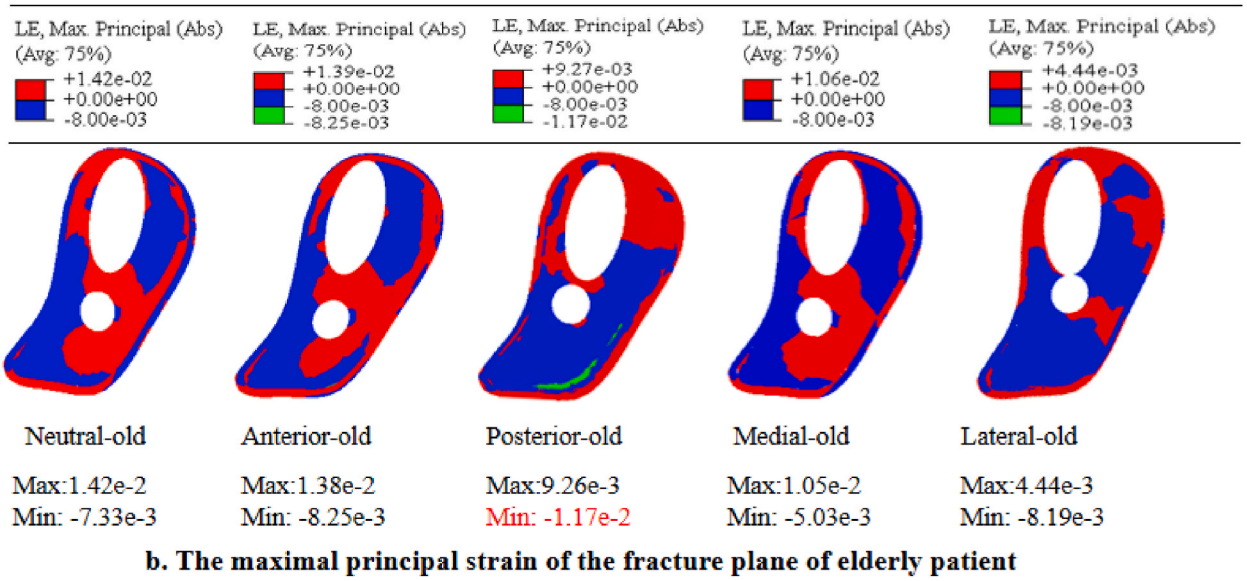

b. The maximal principal strain of the fracture plane of elderly patient

Fig. 9. The maximal principal strain of the fracture plane of young (a) and elderly (b) patient under dynamic analysis with five cortical bone support. The red zone represents the tensional strain, and the blue represents the compressive strain. The green area represents the area likely to be cut out. In the elderly model with posterior cortical bone support, there is a potential risk of fracture plane defects.

dynamic analyses were performed on each model. In static analysis, the von Mises stress distribution, the peak value stress on the femur and the PFNA, and the fracture plane's maximum displacement serve as the main comparative indicators. For the peak value stress of the femur in the young model, the medial cortical support (299.6Mpa, which is significantly lower than the average value of 421.96Mpa) has obvious advantages over the other four cortical supports. While for the old models, the peak value stress under five cortical supports did not show much disparity (the average value 380.38Mpa). In contrast, under the posterior cortical support, the intramedullary nail's stress dramatically increases to 476.54Mpa, which is 1.7 times the average of 280.14Mpa.

We then compared the stress distribution on the femur and PFNA. According to the average fatigue stress of human bones, which is 200Mpa [36–38], stress exceeding 100Mpa was termed a high-stress region. On the femurs of old models with anterior and posterior

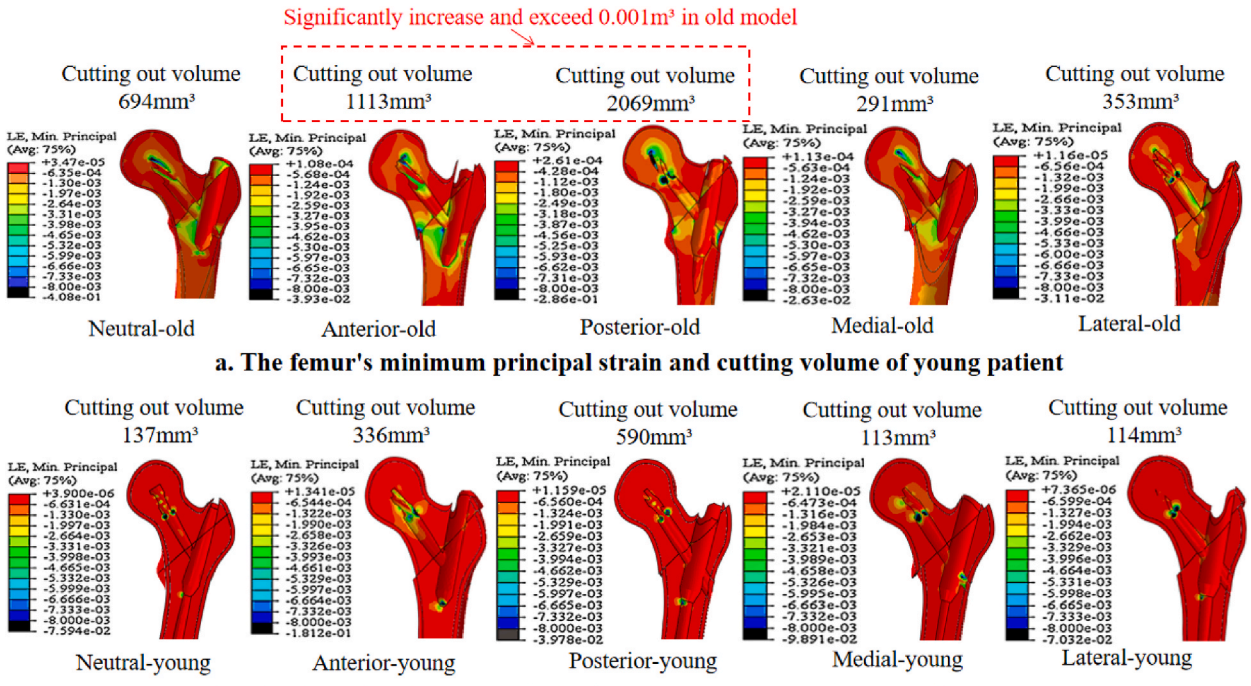

Fig. 10. The femur's minimum principal strain and cutting volume of the young patient (a) and elderly patient (b) in the dynamic analysis with five cortical bone support. In the elderly model, with either anterior or posterior cortical bone support, the volume of cancellous bone resection on the femur exceeds 0.001 m^3.

cortical support, there are substantial red regions (high-stress zones). In both instances, the head-neck fragment is misaligned with the femoral shaft's anterior or posterior cortical bone. Therefore, we concluded that preserving the integrity of the anterior and posterior cortical bone wall is crucial for treating ITFs in elderly patients and sagittal cortical support is recommended in treating ITFs in older people; otherwise, the therapeutic effect would be impaired.

The stress on the PFNA should be as low as feasible to prevent a stress-shielding effect. Stress shielding is a phenomenon where the presence of an implant, such as in orthopedic surgeries, leads to a reduction in the normal stress experienced by the bone, which can result in decreased bone density and strength over time due to the bone's adaptive response to its reduced load-bearing role. Stress shielding may retard fracture healing and increase post-traumatic bone loss [39–41]. The stress distribution varies little amongst the five cortical support types of the young model. However, in the old models, there was a significant stress concentration in the anterior and posterior cortical bone support types, particularly in the intramedullary nail's lower portion. This also indicates that the anterior and posterior cortical bone support should be avoided in the ITF treatment of elderly patients and that the anterior and posterior cortical bone integrity should be prioritized.

The comparison of displacement results reveals that medial cortical support generates the least displacement in both the old and young models, suggesting that this cortical support type is the most stable against external force loading. In the old patients' model, however, the anterior and posterior cortical support generate more fracture plane displacement (3.04 mm and 3.40 mm, respectively) than the medial cortical support (0.55 mm). While in the young model, the fracture plane displacements under anterior and posterior cortical support (0.096 mm and 0.097 mm, respectively) were not markedly different from the medial displacements (0.038 mm).

During the dynamic analysis of the walking cycle, we focused on the cutting volume of the femoral cancellous bone and the range of compressive strain on the fracture plane. In model of younger patients, the neutral and medial cortical supports have a greater compressive strain area, which is favorable for bone healing. In model of older patients, the area of compressive strain cannot be distinguished visually. However, the posterior cortical support contains a considerable green zone (the compressive strain value surpasses −0.8%), indicating that it may be easily broken. There are also green zones in anterior and lateral cortical supports, but these portions are so minute that they may be disregarded. In addition, the volume of cutting under anterior and posterior cortical bone support in the old model (1113 mm^3 and 2069 mm^3, respectively) is much bigger than the amount of cutting under the other three cortical support types. Our simulation findings demonstrate the same phenomenon as static analysis. The age-increasing effect will impact ITF therapy for elderly individuals, and the integrity of anterior and posterior cortical bones should be top considered.

The clinical significance of this study underscores the heightened focus on maintaining the integrity of the anterior and posterior cortical bone wall of the intertrochanteric when treating elderly patients with intertrochanteric fractures. In contrast, younger patients' treatments often primarily rely on medial cortical bone support. This signifies a shift in the emphasis of intertrochanteric fractures' treatment.

5. Limitation

We have detailed the limitations of our study from six aspects. Firstly, regarding the boundary conditions of the finite element analysis model, we simplified aspects such as fixation methods, loading conditions, and muscle force selection for computational efficiency and convergence of simulation results. This simplification might affect the model's accuracy. Secondly, concerning material properties, our finite element model assumed homogenous and isotropic characteristics for bone materials, like the modulus of elasticity. However, in reality, especially for cancellous bone, the material is often heterogeneous and anisotropic, which could impact the simulation results. Additionally, the cortical bone thickness in our model was assumed to be uniformly distributed, whereas in reality, it varies across different parts of the femur, potentially affecting the performance of different cortical bone support.

In terms of age, gender, osteoporosis, and other health factors, the influence of age on bone strength degradation needs further refinement. For instance, the distinction between young and elderly models might vary among individuals, with some entering the bone strength degradation phase earlier. Gender is another critical factor; our models were reconstructed based on female patients since intertrochanteric fractures are three times more common in women than in men [42]. Differences in bone quality parameters and mechanical properties between male and female patients might affect the study's conclusions, necessitating further research. Other health factors, like osteoporosis and osteoarthritis, are also believed to potentially influence the results.

Long-term clinical follow-up data are crucial for validating the model and understanding the long-term effects of treatments. Our model validation, based on the experimental results of Cri et al. [31], would be strengthened by the inclusion of clinical follow-up data. Moreover, our study did not adequately consider the impact of multivariable interactions. For instance, the applicability of our findings to different types of fractures (like A2 and A3, AO/OTA fracture classification), treatment methods (such as different types of screw implants), and daily life activities (such as climbing stairs and bending) requires further validation.

Lastly, regarding the applicability and universality of the model, our conclusions are based on a general model, but patient diversity in terms of race, body type, and physical conditions might influence the applicability of our conclusions. Advancements in personalized modeling techniques could be an effective solution to this issue, enabling individualized surgical analysis and determination of the optimal surgical plan for different patients.

6. Conclusion

In this paper, twenty models for the old and the young with ITFs were established using the finite element method to analyze the performance of five cortical bone supports. Considering the stress distribution, normal strain, and displacement of the femur and PFNA, medial cortical bone support is the optimal ITF reduction therapy for young and elderly individuals. However, age-related changes in bone structure may compromise ITF therapy's efficacy in old people. Current treatment guidelines do not clearly differentiate between therapeutic approaches for intertrochanteric fractures in the elderly compared to the young. Our findings suggest that preserving the integrity and alignment of the anterior and posterior cortical bones is crucial in the treatment of intertrochanteric fractures in the elderly. While the advantage of medial cortical bone support over neutral cortical support is not significantly pronounced, any misalignment of the anterior and posterior cortical bones can severely impact the effectiveness of ITF treatment in elderly patients. Therefore, we conclude that in the treatment of intertrochanteric fractures in the elderly, maintaining the integrity and alignment of the anterior and posterior cortical bone walls is of utmost importance, emphasizing the use of a sagittal support reduction strategy. Our findings have a positive influence on the clinical treatment of ITFs, enhancing surgical treatment effectiveness and postoperative rehabilitation.

Ethics statement

This study has received approval from the Research Ethics Committee of Beijing Jishuitan Hospital, with the permission number GF181020. It should be clarified that although this study has been approved by the ethics committee, it does not constitute a clinical trial. Informed consent has been obtained for the use of patient CT imaging data in this study. We confirm that all patients involved in this study have provided written informed consent in accordance with the journal's requirements, allowing their clinical data to be reported in this manuscript.

Funding

This work was supported by the National Key Research and Development Project (2019YFC0118002), the National Natural Science Foundation of China (NSFC82372386, 61871019), the Natural Science Foundation of Beijing (19L2011), the Capital Health Research and Development of Special (2018-2-2074), and the Beijing Municipal Science and Technology Project (Z201100005420033).

Data availability statement

The data included in this article encompasses clinical data, reference literature data, parameters for model construction, and the results of simulations, all of which are thoroughly detailed in the article. Furthermore, the model files used in the finite element simulation have been uploaded to Mendeley Data. The DOI is as follows: Liu, Jixuan (2024), 'Sagittal Support Rather Than Medial Cortical Support Matters in Geriatric Intertrochanteric Fracture: A Finite Element Analysis Study', Mendeley Data, V1, https://doi.org/10.17632/dmgtpm56db.1.

CRediT authorship contribution statement

Jixuan Liu: Writing – review & editing, Writing – original draft, Methodology, Formal analysis, Data curation, Conceptualization. **Yufeng Ge:** Methodology, Conceptualization. **Yu Wang:** Supervision, Funding acquisition. **Qing Yang:** Data curation. **Sutuke Yibulayimu:** Software. **Xinbao Wu:** Funding acquisition. **Wei Tian:** Supervision. **Chao Shi:** Validation. **Yanzhen Liu:** Visualization. **Minghui Yang:** Resources, Conceptualization.

Declaration of competing interest

The authors declare that they have no known competing financial interests or personal relationships that could have appeared to influence the work reported in this paper.

Abbreviation

ITF	Intertrochanteric fracture
PFNA	Proximal femoral nail anti-rotation
FE	Finite element
AO/OTA	Association of Orthopaedic/Orthopaedic Trauma Association
NURBS	Non-uniform rational B-spline

References

[1] L. Wang, X.G. Cheng, Y.B. Su, K. Brown, L. Xu, et al., Sex-related variations in cortical and trabecular bone of the femoral neck in an elderly Chinese population, Osteoporos. Int. 28 (2017) 2391–2399.
[2] D.K. Mueller, A. Kutscherenko, H. Bartel, A. Vlassenbroek, P. Ourednicek, J. Erckenbrecht, Phantom-less QCT BMD system as screening tool for osteoporosis without additional radiation, Eur. J. Radiol. 79 (2011) 375–381.
[3] J. Kaesmacher, H. Liebl, T. Baum, J.S. Kirschke, Bone mineral density estimations from routine multidetector computed tomography: a comparative study of contrast and calibration effects, J. Comput. Assist. Tomogr. 41 (2017) 217–223.
[4] S. Eberle, C. Gerber, G. von Oldenburg, S. Hungerer, P. Augat, Type of hip fracture determines load share in intramedullary osteosynthesis, Clin. Orthop. Relat. Res. 467 (2009) 1972–1980.
[5] V. Breuil, C.H. Roux, J. Testa, C. Albert, M. Chassang, et al., Outcome of osteoporotic pelvic fractures: an underestimated severity. Survey of 60 cases, Joint Bone Spine 75 (2008) 585–588.
[6] H. Zhuang, Y. Li, J. Lin, D. Cai, S. Cai, et al., Cortical thickness in the intertrochanteric region may be relevant to hip fracture type, BMC Muscoskel. Disord. 18 (2017) 305.
[7] S. Eberle, C. Gerber, G. von Oldenburg, F. Hogel, P. Augat, A biomechanical evaluation of orthopaedic implants for hip fractures by finite element analysis and in-vitro tests, Proc. Inst. Mech. Eng. H 224 (2010) 1141–1152.
[8] W. Ekstrom, G. Nemeth, E. Samnegard, N. Dalen, J. Tidermark, Quality of life after a subtrochanteric fracture: a prospective cohort study on 87 elderly patients, Injury 40 (2009) 371–376.
[9] I. Saarenpaa, T. Heikkinen, P. Jalovaara, Treatment of subtrochanteric fractures. A comparison of the Gamma nail and the dynamic hip screw: short-term outcome in 58 patients, Int. Orthop. 31 (2007) 65–70.
[10] L. Zheng, X. Chen, Y. Zheng, X. He, J. Wu, Z. Lin, Cement augmentation of the proximal femoral nail antirotation for the treatment of two intertrochanteric fractures - a comparative finite element study, BMC Muscoskel. Disord. 22 (2021) 1010.
[11] K. H, Mechanics of the treatment of hip injuries, Clin. Orthop. Relat. Res. 146 (1980) 53–61.
[12] Y. Gotfried, S. Kovalenko, D. Fuchs, Nonanatomical reduction of displaced subcapital femoral fractures (Gotfried reduction), J. Orthop. Trauma 27 (2013) e254–e259.
[13] Y.Q.C.S. Zhang, Mechanism of "Gotfried reduction'' in femoral neck fracture, J. Orthop. Trauma 27 (12) (2013) e291.
[14] S.M. Chang, Y.Q. Zhang, Z. Ma, Q. Li, J. Dargel, P. Eysel, Fracture reduction with positive medial cortical support: a key element in stability reconstruction for the unstable pertrochanteric hip fractures, Arch. Orthop. Trauma. Surg. 135 (2015) 811–818.
[15] S.M. Chang Yqz, S.C. Du, Z. Ma, S.J. Hu, X.Z. Yao, W.F. Xiong, Anteromedial cortical support reduction in unstable pertrochanteric fractures: a comparison of intra-operative fluoroscopy and post-operative three dimensional computerised tomography reconstruction, Int. Orthop. 42 (1) (2018) 183–189.
[16] Q. Shao, Y. Zhang, G.X. Sun, C.S. Yang, N. Liu, et al., Positive or negative anteromedial cortical support of unstable pertrochanteric femoral fractures: a finite element analysis study, Biomed. Pharmacother. 138 (2021) 111473.
[17] W. Mao, S.M. Chang, Y.Q. Zhang, Y. Li, S.C. Du, et al., Positive medial cortical support versus anatomical reduction for trochanteric hip fractures: finite element analysis and biomechanical testing, Comput. Methods Progr. Biomed. 234 (2023) 107502.
[18] J. Li Lz, H. Zhang, P. Yin, M. Lei, G. Wang, S. Wang, P. Tang, Effect of reduction quality on post-operative outcomes in 31-A2 intertrochanteric fractures following intramedullary fixation: a retrospective study based on computerised tomography findings, Int. Orthop. 43 (8) (2019) 1951–1959.
[19] K. Ramachandran Kkam, A.V. Sankar, Critical analysis of factors determining mechanical failures in proximal femoral nailing, Int. J. Res. Orthop. 5 (2) (2019) 275–282.
[20] T.A. Russell Rs, Pertrochanteric hip fractures: time for change, J. Orthop. Trauma 25 (4) (2011) 189–190.
[21] K.A. Ward, J.E. Adams, T.N. Hangartner, Recommendations for thresholds for cortical bone geometry and density measurement by peripheral quantitative computed tomography, Calcif. Tissue Int. 77 (2005) 275–280.
[22] B.L. Riggs, L.J. Melton Iii, R.A. Robb, J.J. Camp, E.J. Atkinson, et al., Population-based study of age and sex differences in bone volumetric density, size, geometry, and structure at different skeletal sites, J. Bone Miner. Res. 19 (2004) 1945–1954.
[23] B.G.J. Seral, J. Cegoino, M. Doblare, F. Seral, 3D finite element analysis of the gamma nail and DHS plate in trochanteric hip fractures, Hip Int. 14 (2004) 18–23.
[24] A. Furui, N. Terada, K. Mito, Mechanical simulation study of postoperative displacement of trochanteric fractures using the finite element method, J. Orthop. Surg. Res. 13 (2018) 300.
[25] L. Yin, Z. Xu, L. Wang, W. Li, Y. Zhao, et al., Associations of muscle size and density with proximal femur bone in a community dwelling older population, Front. Endocrinol. 11 (2020) 503.
[26] R.Y.W.X. Zhong, E.Y. Liao, et al., Relationship between age-related bone mass of the lumbar spine and skeletal size and their effects on the diagnosis of osteoporosis in women, Chin. J. Osteoporos. 18 (2) (2012) 99–105.

[27] W.C.P.S. Hayes, P.K. Zysset, Biomechanics of fracture risk prediction of the hip and spine by quantitative computed tomography, Radiol. Clin. 29 (1) (1991) 1–18.
[28] A.N.L. Polikeit, S.J. Ferguson, et al., The effect of cement augmentation on the load transfer in an osteoporotic functional spinal unit (finite-element analysis), Spine 28 (10) (2003) 991–996.
[29] H.H. Bayraktar, E.F. Morgan, G.L. Niebur, G.E. Morris, E.K. Wong, T.M. Keaveny, Comparison of the elastic and yield properties of human femoral trabecular and cortical bone tissue, J. Biomech. 37 (2004) 27–35.
[30] C. Lee, B. Kelley, A. Gurbani, A.I. Stavrakis, Strategies for pertrochanteric fracture reduction and intramedullary nail placement: technical tips and tricks, J. Am. Acad. Orthop. Surg. 30 (2022) 867–878.
[31] L.V.M. Cristofolini, A. Cappello, A. Toni, Mechanical validation of whole, Mechanical validation of whole bone composite femur models, J. Biomech. 29 (1996) 525–535.
[32] J.C.C.E.J. Lotz, W.C. Hayes, Stress distributions within the proximal femur during gait and falls: implications for osteoporotic fracture, Osteoporos. Int. 5 (4) (1995) 252–261.
[33] G. Bergmann, A. Bender, J. Dymke, G. Duda, P. Damm, Standardized loads acting in hip implants, PLoS One 11 (2016) e0155612.
[34] P.B.J. Augat, S. Schorlemmer, T. Henke, M. Peraus, L. Claes, Shear movement at the fracture site delays healing in a diaphy seal fracture model, J. Orthop. Res. 21 (2003) 1011–1017.
[35] D.L.K.T. Kopperdahl, Yield strain behavior of trabecular bone, J. Biomech. 31 (1998) 601–608.
[36] J. Zpwxc, The accumulation of fatigue microdamage in human cortical bone of two different ages in vitro, Clin. Biomech. 11 (7) (1996) 365–375.
[37] J. Liu, K. Xu, C. Zhao, G. Zhu, Y. Wang, et al., Experimental and finite element analysis studies of a reduction-force reducing traction method for pelvic fracture surgeries, Medicine in Novel Technology and Devices 13 (2022).
[38] J. Liu, Y. Yan, K. Xu, C. Zhao, Y. Wang, et al., Biomechanical analysis of pelvic holding pathways and strategies for use of the steinmann pin in pelvic fracture reduction, Comput. Biol. Med. 152 (2023) 106310.
[39] V.K. Ganesh, K. Ramakrishna, D.N. Ghista, Biomechanics of bone-fracture fixation by stiffness-graded plates in comparison with stainlesssteel plates, Biomed. Eng. Online 4 (2005) (2005) 46.
[40] Y. Fan, K. Xiu, H. Duan, M. Zhang, Biomechanical and histological evaluation of the application of biodegradable poly-L-lactic cushion to the plate internal fixation for bone fracture healing, Clin. Biomech. 23 (Suppl. 1) (2008) S7–S16.
[41] P. Augat, L. Claes, Increased cortical remodeling after osteotomy causes posttraumatic osteopenia, Bone 43 (2008) 539–543.
[42] N. Veronese, S. Maggi, Epidemiology and social costs of hip fracture, Injury 49 (2018) 1458–1460.